Backscattering of Electrons from 3.2 to 14 MeV*

TATSUO TABATA
Radiation Center of Osaka Prefecture, Sakai, Osaka, Japan
(Received 30 March 1967)

Monoenergetic electrons of energies from 3.2 to 14 MeV provided by a linear accelerator have impinged normally on thick solid targets. Backscattered electrons have been detected by an ionization chamber, the multiplication factor of which was calibrated with a Faraday chamber as a function of average energy per backscattered electron. Angular distributions of backscattered electrons measured for a total of seven targets, effectively semi-infinite and ranging in atomic numbers from 4 to 92, show a trend similar to Dressel's result. However, the backscattering coefficients obtained are lower than his values and are consistent with those reported by other previous authors. Variations of angular distribution and backscattering coefficient with target thickness also have been investigated for Cu, Ag, and Au targets at an incident energy of 6.1 MeV. Some of the angular distributions observed were compared with results of a simple calculation proposed by the author, and an interpretation has been given that the relative contribution of sidescattering compared with that of diffusion increases with increasing energy in the region considered. Backscattering coefficients for the thinnest targets of lower atomic numbers level off toward a nonzero intercept similar to Cohen and Koral's lower-energy result. This tendency is considered to be caused by the contribution of energetic secondary electrons. The backscattering coefficient $\eta(E_0, Z, \infty)$ of electrons incident on the semi-infinite target of atomic number Z with kinetic energy E_0 above 1 MeV is expressed by an empirical equation $\eta(E_0, Z, \infty) = 1.28 \exp[-11.9Z^{-0.65}(1+0.103Z^{0.37}E_0^{0.65})]$ (E_0 in MeV), appreciable deviations from experimental data occurring only for $Z \leq 6$ and $Z/E_0 \lesssim 2$ MeV^{-1}.

I. INTRODUCTION

WHEN a beam of fast electrons impinges on a thick solid target, some electrons emerge from the incident surface. These back-directed electrons are composed of two groups: secondary electrons and backscattered electrons.[1,2] Experimentally, all electrons emitted with energies less than 50 eV are usually associated with the secondary emission mechanism, and those with higher energies are regarded as backscattered electrons. While the number of backscattered electrons below 50 eV may well be neglected, the number of energetic secondary electrons above 50 eV is considered to become appreciable in some cases. The latter are, however, difficult to distinguish from the backscattered electrons proper.

Individual elementary processes experienced by electrons in passing through bulk matter are rather well understood, and most of the transport problem of electrons can be solved by calculation. Theoretical treatments of the backscattering phenomenon, for example by diffusion theory[3,4] and large-angle single elastic scattering theory,[1] have been tried for incident electron energies below 2 MeV; however, they have met with only limited success because of their severe approximations. An attempt to get the solution of the integral equation derived from invariant imbedding also has been confined to incident energies in the keV region,[5] since scattering cross sections take on considerably complicated forms for higher energies. Though application of the Monte Carlo method is a promising alternative approach, it has been restricted to the calculation of total backscattering coefficient for energies below 4 MeV.[6] In the energy region higher than this, there are neither theoretical treatments nor sufficient experimental data to understand the whole aspect of backscattering. Harder and Ferbert[7] measured the total backscattering coefficient in the energy range 8–22 MeV. Dressel observed the angular distribution of backscattered electrons and the backscattering coefficient[8] as well as the energy distribution of these electrons[9] for incident energies 0.5–10 MeV. Values of the backscattering coefficient reported by him were appreciably higher than the results of previous authors.[2,7,10–12] More experimental data are required for energies above a few MeV, not only to resolve the discrepancy between the result of Dressel and other previous authors, but also to throw new light on the relative importance of contributing processes resulting from accumulation of elementary encounters. Such information may be useful for establishing a new theoretical approach.

In the experiment described here, the angular distribution of backscattered electrons and the backscattering coefficient were measured for Cu, Ag, and Au targets of various thicknesses at the incident energy of 6.08 MeV, and for Be, C, Al, Cu, Ag, Au, and U targets of

* This work was supported by a grant from the Science and Technology Agency of the Japanese Government.

[1] T. E. Everhart, J. Appl. Phys. **31**, 1483 (1960).
[2] K. A. Wright and J. G. Trump, J. Appl. Phys. **33**, 687 (1962).
[3] H.-W. Thümmel, Z. Physik **179**, 116 (1964).
[4] A fairly complete list of references dealing with backscattering of electrons has been given by Dressel (Refs. 8 and 9), so that only one example of each type of paper is cited here for every similar treatment.
[5] R. F. Dashen, Phys. Rev. **134**, A1025 (1964).
[6] J. F. Perkins, Phys. Rev. **126**, 1781 (1962).
[7] D. Harder and H. Ferbert, Phys. Letters **9**, 233 (1964).
[8] R. W. Dressel, Phys. Rev. **144**, 332 (1966).
[9] R. W. Dressel, Phys. Rev. **144**, 344 (1966).
[10] H. Frank, Z. Naturforsch. **14a**, 247 (1959).
[11] A. J. Cohen and K. F. Koral, National Aeronautics and Space Administration Technical Note TND-2782, 1965 (unpublished).
[12] In addition to the references listed by Dressel, the author has noticed the following works that report values of backscattering coefficient measured for incident energies in the region 0.6–1.2 MeV. P. Ya. Glazunov and V. G. Guglya, Dokl. Akad. Nauk SSSR **159**, 632 (1964); and D. H. Rester and W. J. Rainwater Jr., Nucl. Instr. Methods **41**, 51 (1966).

effectively semi-infinite thickness in the energy range 3.24–14.1 MeV. Angular distributions observed are compared with results of a simple calculation proposed by the author, and general trends of the contributing processes are discussed. The relation between relative backscattering coefficient and target thickness was fitted with an empirical relation given by Koral and Cohen.[13] An empirical equation was found to express the backscattering coefficient for a semi-infinite target as a function of incident energy and target atomic number.

II. EXPERIMENTAL

A. General Description

Consider the backscattering of electrons with incident kinetic energy E_0 from a target of atomic number Z and thickness t. The differential backscattering coefficient $d\eta(\theta; E_0, Z, t)$ is defined as the number of electrons, per incident electron, backscattered through the angle θ into the solid angle $d\Omega$. Experimentally it is determined from

$$d\eta(\theta; E_0, Z, t) = i_b(\theta)\, d\Omega / I_0, \quad (1)$$

where $i_b(\theta)$ is the backscattered electron current into the unit solid angle at θ, and I_0 is the incident current. In the present experiment the target current I_t was measured instead of I_0 (when the target was thinner than the maximum range of electrons, a target assembly backed with a Faraday cup was used, and its total current was identified with I_t). The relation between them is expressed by

$$I_0 = I_t + I_b + I_s, \quad (2)$$

where I_b is the total backscattered current into the backward hemisphere:

$$I_b = \int_{\pi/2}^{\pi} \int_0^{2\pi} i_b(\theta)\, \sin\theta d\theta d\varphi, \quad (3)$$

and I_s is the secondary emission current from the target. From these relations the total backscattering coefficient $\eta(E_0, Z, t)$ is given by

$$\eta(E_0, Z, t) = \rho(1-\delta)/(1+\rho), \quad (4)$$

where ρ denotes the ratio I_b/I_t and δ is the secondary-emission coefficient I_s/I_0. In this experiment an ionization chamber was used for detecting backscattered electrons, and it was insensitive to the secondary electrons. Then $i_b(\theta)$ is expressed in terms of the ionization current $I_i(\theta)$, observed at the scattering angle θ, by

$$i_b(\theta) = I_i(\theta)/f\omega, \quad (5)$$

where f is the multiplication factor of the ionization chamber, and ω is the solid angle subtended at the target by the aperture of the detector collimator.

[13] K. F. Koral and A. J. Cohen, National Aeronautics and Space Administration Technical Note TND-2907, 1965 (unpublished).

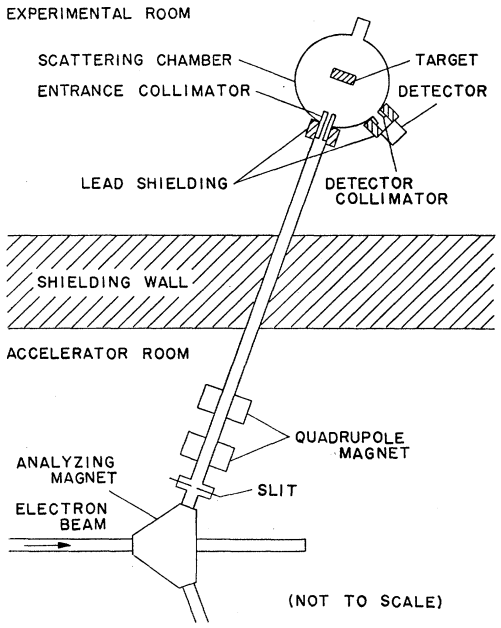

FIG. 1. Schematic diagram of the experimental arrangement.

B. Electron Beam

The experimental arrangement is shown schematically in Fig. 1. The electron beam from the linear accelerator of the Radiation Center of Osaka Prefecture[14] was deflected into the experimental area by an analyzing magnet. A pair of quadrupole magnets focused the beam on the entrance collimator of the scattering chamber placed 5.5 m away. The collimator was made of copper and was 160 mm in length. The beam at the target had an energy spread of about 1%, an angular divergence less than 0.05°, and a diameter of 6.5 mm. The energy scale of the analyzing magnet was calibrated within an error of 1.1% by measuring the conversion-electron line of Cs^{137} and the threshold of the $Cu^{63}(\gamma, n)$ reaction. The target current used was of the order 0.01–0.1 μA.

C. Scattering Chamber

The scattering chamber[15] consists of a fixed lid and a rotatable cylindrical box, each 50 cm i.d. and 15 cm high and made of stainless steel. The incident beam enters horizontally through the port at the side of the lid. The measuring port is attached to the box with a dip of 20° from the horizontal plane. The rotation of the box can be performed under vacuum with remote control of a drive motor. The angular position θ_0 of the measuring port, projected in the horizontal plane, may be known to 0.2° at the control panel. The scattering

[14] S. Okabe *et al.*, Ann. Rept. Radiation Center Osaka Prefect. **3**, 47 (1962).

[15] T. Tabata, S. Okabe, and R. Ito, Ann. Rept. Radiation Center Osaka Prefect. **5**, 60 (1964).

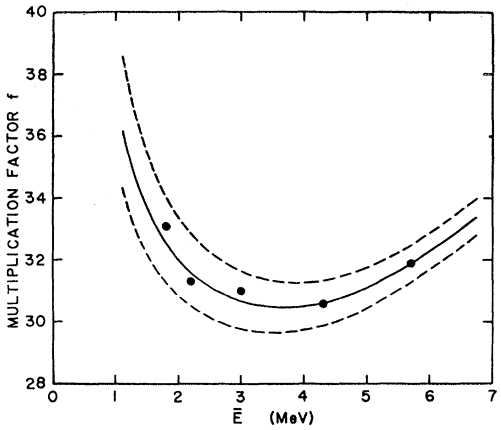

FIG. 2. Multiplication factor f of the ionization chamber as a function of average energy $\bar{E}$ per backscattered electron. Dashed curves show the limit of possible error due to uncertainty in the correction of Faraday chamber efficiency.

angle θ is given by the equation

$$\cos\theta = \cos 20^\circ \cos\theta_0. \quad (6)$$

Observation is possible with this apparatus in the continuous range of scattering angle 20–160° on both sides of the incident beam. The vacuum in the scattering chamber was of the order of 10^{-5} mm Hg and was scarcely affected by rotation. The target was hung with a rotatable supporting rod from the center of the lid and insulated so that the target current could be measured.

After passing through a detector collimator and through a 3.5-mg/cm² Mylar window in the measuring port, the backscattered electrons entered the ionization chamber. The detector collimator was made of copper and had a conical taper matching the solid-angle cone subtended at the center of the target surface. The solid angle of detection was calculated from geometrical dimensions to be 1.92×10^{-4} sr.

D. Targets and Target Assembly

As far as backscattering is concerned, a target of thickness greater than half of the practical range of incident electrons can be considered effectively semi-infinite.[11,13] Such a target is called here a "semi-infinite target," and a "thin target" is defined as one thinner than half the practical range. Semi-infinite targets used were Be, C, Al, Cu, Ag, Au, and U. They were solid disks of diameters 40–80 mm and of thickness larger than 8.1 g/cm², except for the Be target, which was 1.8 g/cm² thick, permitting measurement at the three lowest energies used in this experiment. Thin targets were Cu, Ag, and Au in the form of foil or plate 40 mm in diameter. All the targets were of purity better than 99.5%. The target was mounted on the supporting rod by using a ring-shaped copper holder and a ceramic insulator. When the target was thinner than the maximum range of incident electrons, it was backed with an aluminum Faraday cup having an entrance hole 11 mm in diameter and 35 mm in depth. In every case the target was placed perpendicular to the beam, the center of the incident surface being laid at the center of the scattering chamber.

E. Ionization Chamber and Measurements

The ionization chamber was of the x-ray compensation type developed by Van de Graaff *et al.*[16] The design was modified in dimensions to meet the present experimental conditions. The charge collector was an aluminum plate 60 mm in diameter and 30 mm thick, sandwiched between two aluminum foils 27 mg/cm² thick. The gap between the charge collector and each of the foils was about 4 mm, the cavities being filled with air at atmospheric pressure. By applying high voltages of opposite polarities to the foils, x-ray background originating from the entrance collimator and the target was much reduced with this arrangement. In order to measure the uncompensated portion of the background, a remotely controlled shutter was provided at the entrance of the ionization chamber. It consisted of a copper plate 40 mm in diameter and 10 mm thick and could prevent electrons from entering the ionization chamber.

The ionization current from the chamber was amplified with a picoammeter and fed to a current integrator, while the target current was measured with another current integrator. The ionization current during the measurement was of the order 10^{-7}–10^{-4} μA. Since the accelerator was pulsed, possible saturation of the ionization chamber was examined and found not to occur up to an ionization current of about 5×10^{-2} μA under the duty of 5×10^{-5} used. In order to minimize the effect of errors in angular alignment of the scattering chamber and the target surface, measurements were made on both sides of the incident beam and average values were adopted.

The multiplication factor f of the ionization chamber depends on the energy spectrum of backscattered electrons and is a function of E_0, Z, t, and θ. In the present work it was assumed to be determined uniquely as a function of average energy $\bar{E}(E_0, Z)$ per backscattered electron from the semi-infinite target, by neglecting its dependence on t and θ. Values of $\bar{E}(E_0, Z)$ were estimated with the method described in Appendix A. Since specific ionization produced by the electron is a rather slowly varying function of energy above about 1 MeV,[17] the error caused by this assumption is expected not to be serious in most cases, and is included in possible systematic errors described in Sec. III C.

On the above assumption, the calibration of f was made by comparing the value of fI_b [see Eqs. (3) and (5)] obtained with the ionization chamber with the value of I_b measured by using a Faraday chamber. For

[16] R. J. Van de Graaff, W. W. Buechner, and H. Feshbach, Phys. Rev. 69, 452 (1946).
[17] W. C. Barber, Phys. Rev. 97, 1071 (1955).

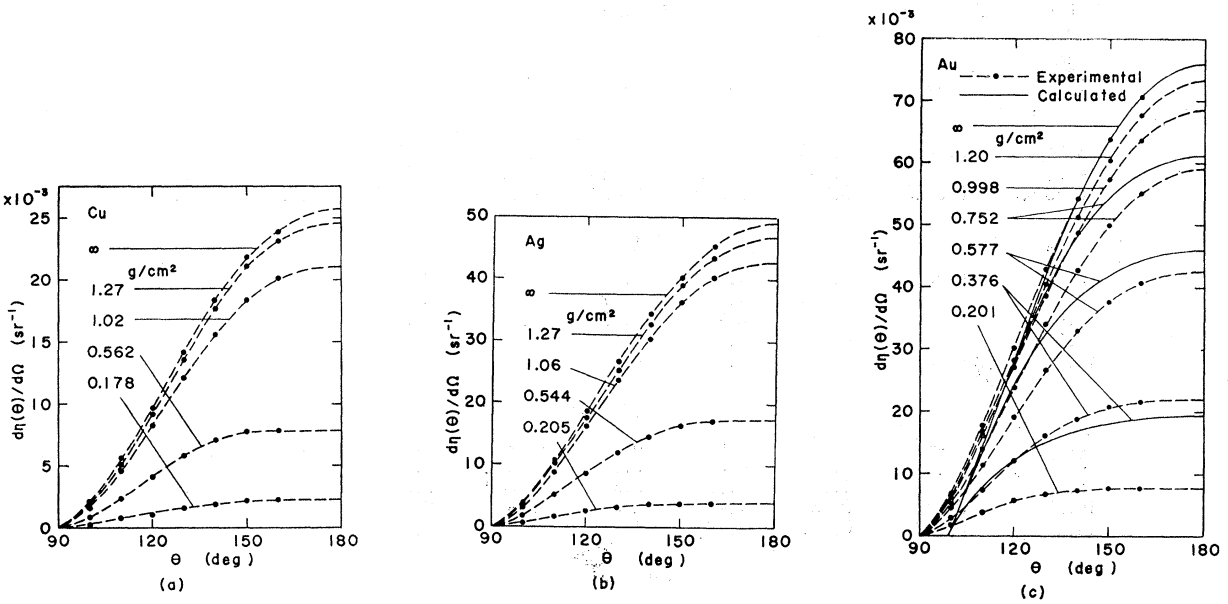

FIG. 3. Angular distributions of backscattered electrons from targets of various thicknesses. The incident electron energy is 6.08 MeV. (a), (b), and (c) show the case of Cu, Ag, and Au targets, respectively. The solid curves in (c) are calculated distributions normalized to the experimental value for the semi-infinite target at 180° (see Sec. IV A2).

this comparison the semi-infinite Au target was used, because the comparatively high backscattering coefficient for it made the measurement possible without amplification at the detector stage.

The Faraday chamber used in the calibration consisted of a brass container and an aluminum collector 60 mm in diameter and 30 mm thick. It was attached to the measuring port of the scattering chamber and pumped by the same vacuum system. In using the Faraday chamber, the secondary electrons from the target were prevented from reaching the collector by a potential applied to the detector collimator, while they were cutoff by the window foil in the measurement with the ionization chamber. A correction of Faraday chamber efficiency for backscattering and secondary emission from the collector was made by using the values of respective coefficients for electrons of energy $\bar{E}(E_0, 79)$. Values of the backscattering coefficient for Al were obtained by interpolating the data of Wright and Trump[2] and of Harder and Ferbert[18]; concerning the secondary emission coefficient, a description will be given in Sec. II G. The total correction of efficiency ranged from 4.1 to 8.9%. The calibration curve obtained in this way is shown in Fig. 2.

F. Background

The x-ray background remaining uncompensated in the ionization chamber was measured under each condition by closing the shutter as described before. There was smaller background of another type, principally due to secondary electrons produced near the measuring port of the scattering chamber by bremsstrahlung x rays from the entrance collimator. Since this background could not be measured by closing the shutter, it was studied for each incident energy without the target. The net signal was obtained by subtracting the backgrounds of both types after proper normalization. The total background was always highest at 160°, where the ratio of background to signal was about 0.5–20% depending on E_0 and Z.

A small fraction of the background caused by target bremsstrahlung also could not be measured by closing the shutter, because of the attenuation of bremsstrahlung intensity in it. The size of this fraction was investigated under the most unfavorable conditions by putting an extra copper plate between the ionization chamber and the shutter, and was found to be less than 1% of the signal.

When the Faraday chamber detector was used for calibration the background was observed by inserting an aluminum plug 35 mm long in the detector collimator. The ratio of background to signal at 160° varied from 2 to 12% with increasing E_0.

G. Secondary Electrons

In order to obtain the backscattering coefficient from Eq. (4), a knowledge is required of the secondary-emission coefficient δ for the targets used. It was measured for the semi-infinite targets with the aid of a ring-shaped electrode attached to the incident side of the target. In this measurement the beam current was monitored by measuring the backscattered electrons with the ionization chamber at 160°, and the dependence of target current on negative bias voltage applied to the electrode was observed. Determination of δ from this measurement presumes the converse situation: that

[18] D. Harder (private communication). Results reported in Ref. 7 have been corrected in this communication to slightly smaller values.

TABLE I. Differential backscattering coefficients $d\eta(\theta; E_0, Z, \infty)/d\Omega$ for semi-infinite targets. Values are given in 10^{-3}/sr.

E_0 (MeV)	100	110	120	θ(°) 130	140	150	160	Error ±(%)
				Be ($Z=4$)				
3.24	0.168	0.416	0.636	0.778	0.926	0.977	1.04	13
4.09	0.125	0.347	0.518	0.640	0.753	0.774	0.791	13
6.08	0.0940	0.263	0.349	0.469	0.527	0.544	0.537	11
				C ($Z=6$)				
3.24	0.325	0.862	1.40	1.94	2.40	2.76	3.04	13
4.09	0.252	0.682	1.12	1.49	1.78	2.04	2.18	13
6.08	0.162	0.482	0.738	0.963	1.13	1.24	1.33	11
10.1	0.180	0.333	0.558	0.665	0.812	0.860	0.904	8.5
14.1	0.186	0.300	0.412	0.596	0.761	0.819	0.821	8.3
				Al ($Z=13$)				
3.24	1.24	3.25	5.65	8.17	10.4	12.5	13.9	13
4.09	0.974	2.64	4.38	6.53	8.49	10.0	11.2	13
6.08	0.696	1.61	2.70	3.83	4.78	5.58	6.13	11
10.1	0.312	0.939	1.49	2.06	2.45	2.88	3.16	8.5
14.1	0.270	0.671	1.18	1.53	1.80	2.15	2.24	8.3
				Cu ($Z=29$)				
3.24	3.82	9.95	17.7	25.8	33.3	39.8	44.6	11
4.09	3.07	8.03	14.5	21.1	27.1	32.7	36.4	12
6.08	2.12	5.56	9.71	14.2	18.3	21.8	23.9	9.8
10.1	1.07	3.00	5.25	7.63	9.63	11.5	13.0	8.1
14.1	0.741	1.89	3.48	5.17	6.43	7.62	8.63	8.5
				Ag ($Z=47$)				
3.24	6.59	17.2	30.2	43.5	55.4	65.6	73.1	10
4.09	5.50	14.9	26.1	37.0	47.5	55.9	62.9	10
6.08	3.94	10.8	18.6	26.8	34.3	40.3	45.3	8.7
10.1	2.24	6.09	10.6	15.3	19.5	22.9	26.1	7.6
14.1	1.56	4.03	6.92	9.96	12.7	15.2	17.1	8.7
				Au ($Z=79$)				
3.24	10.2	26.1	44.5	62.9	79.6	93.3	103	8.9
4.09	9.12	23.6	40.1	57.2	72.0	85.0	93.7	8.0
6.08	6.80	17.7	30.2	42.9	54.3	63.7	70.6	7.4
10.1	4.09	10.8	18.5	26.2	33.6	39.7	44.0	7.2
14.1	2.71	7.12	12.4	17.5	22.5	27.0	29.8	9.1
				U ($Z=92$)				
3.24	11.4	29.4	50.4	71.9	90.5	105	117	7.3
4.09	9.88	25.5	43.5	61.6	78.0	90.6	101	7.1
6.08	7.52	19.6	33.4	47.5	60.2	70.7	78.1	6.9
10.1	4.09	11.3	19.7	28.3	36.1	42.7	47.3	7.7
14.1	2.56	7.26	12.9	18.7	24.0	28.3	31.7	9.2

the backscattering coefficient is known. For this purpose, however, it was sufficient to use values of the backscattering coefficient obtained by assuming approximate values of δ.

A trend of slight decrease of δ with increasing incident energy was observed, especially for high-atomic-number targets. This is considered to be due to the decrease with energy of the number of backscattered electrons that also cause secondary emission. Dobretsov and Matskevich[19] used the relation

$$\delta = \delta_0(1+\beta\eta), \qquad (7)$$

where δ_0 is the secondary-emission coefficient due to incident electrons, β is the efficiency of backscattered electrons in forming secondary electrons, and η is the total backscattering coefficient. The value of β was found to be close to unity for the present energy region; those of δ_0, whose dependence on incident energy could be neglected for the present purpose, were about 2.1% for Be, 1.5% for C, 2.1% for Al, 2.8% for Cu, 3.4% for Ag, 4.3% for Au, and 3.2% for U. The values of δ for thin targets were estimated from Eq. (7); this relation and the value of δ_0 for Al were used also for determining the correction factor of the Faraday chamber efficiency.

The bremsstrahlung x rays produced in the target may also emit secondary electrons, mainly from the

[19] L. N. Dobretsov and T. L. Matskevich, Zh. Techn. Fiz. 27, 734 (1957) [English transl.: Soviet Phys.—Tech. Phys. 2, 663 (1957)].

forward surface of the target. When this yield is appreciable, it should be taken into account in Eq. (4). However, it was experimentally confirmed to be less than 0.5% of the target current.

III. RESULTS

A. Angular Distribution

1. Variation with Thickness

The differential backscattering coefficients observed for thin targets at the incident energy of 6.08 MeV are shown in Fig. 3 together with results for the semi-infinite targets of the same atomic numbers. Extrapolated values at 180°were obtained in a plot with a $\cos\theta$ scale, since the narrowing of intervals between observed points toward 180° in this plot made the extrapolation easier.

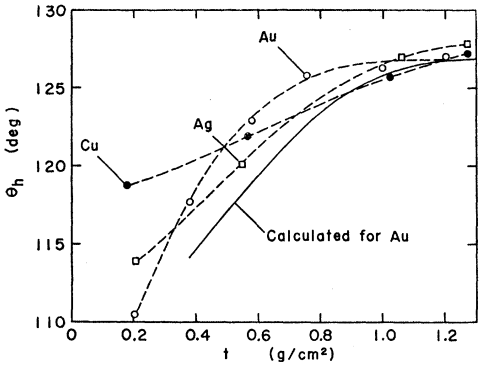

FIG. 4. Dependence of half-value angle θ_h on target thickness t. The incident-electron energy is 6.08 MeV. The solid curve shows the calculated result for Au (see Sec. IV A2).

In order to compare shapes of angular distributions, it is convenient to use the half-value angle θ_h at which the differential backscattering coefficient $d\eta(\theta)/d\Omega$ has fallen to $\frac{1}{2}$ of the value at the maximum (see Fig. 5). In Fig. 4, θ_h is plotted as a function of target thickness t. The distribution becomes broader (θ_h decreases) with decreasing thickness similarly to the case of 1.75-MeV incident energy studied by Frank.[10] There can be seen a trend that the difference in θ_h at the lowest and the highest thickness is larger for higher-Z targets.

2. Semi-Infinite Targets

The differential backscattering coefficients were measured for semi-infinite targets at incident energies: 3.24, 4.09, 6.08, 10.1, and 14.1 MeV, and the results are summarized in Table I. The relative angular distributions for Be and U are illustrated in Fig. 5, and the variation of θ_h with incident energy E_0 is shown in Fig. 6. For targets of atomic number $Z\geq 29$, θ_h is almost independent of both E_0 and Z; for $Z\leq 13$, it decreases with increasing E_0 and increases with increasing Z. This is qualitatively in agreement with Dressel's result.[8]

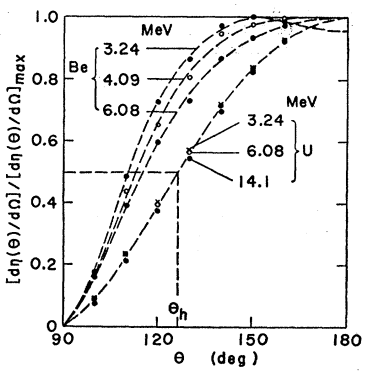

FIG. 5. Angular distributions of backscattered electrons for various incident energies in the cases of semi-infinite Be and U targets. The curves are normalized to unity at the maximum. (Values of energy 3.24 and 6.08 MeV attached to the angular distributions for Be should be interchanged.)

However, the values of θ_h for $Z\leq 13$ observed in the present experiment are in most cases appreciably smaller than his values. A possible reason for this will be discussed in the next section.

B. Total Backscattering Coefficient

1. Dependence on Thickness

The ratio of total backscattering coefficient $\eta(E_0, Z, t)$ for a target of thickness t to the coefficient $\eta(E_0, Z, \infty)$ for a semi-infinite target of the same atomic number is shown in Fig. 7 as a function of t for the case of 6.08-MeV incident energy. It can be seen that the ratio rises faster with mass thickness t for higher-Z targets, similarly to the case of incident energies 0.6–1.8 MeV investigated by Cohen and Koral.[11]

2. Semi-Infinite Targets

The total backscattering coefficients obtained for semi-infinite targets are given in Table II and shown in

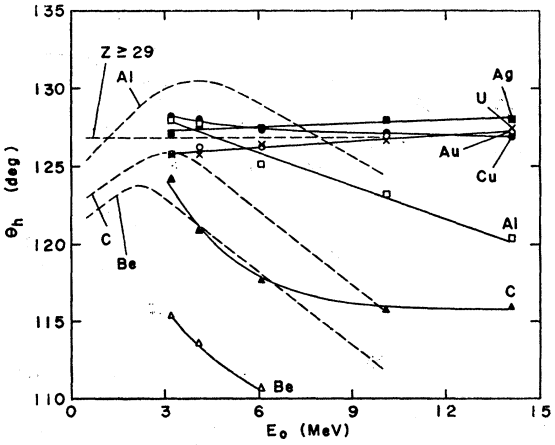

FIG. 6. Variation of half-value angle θ_h for semi-infinite targets with incident energy E_0. Dashed line, Dressel (Ref. 8).

TABLE II. Total backscattering coefficients $\eta(E_0, Z, \infty)$ for semi-infinite targets. Values are expressed in %.

E_0 (MeV)	Target Be	C	Al	Cu
3.24	0.37±0.05	0.92±0.12	4.0 ±0.5	12.5 ±1.4
4.09	0.30±0.04	0.70±0.09	3.2 ±0.4	10.2 ±1.2
6.08	0.21±0.02	0.45±0.05	1.8 ±0.2	6.84±0.67
10.1	...	0.32±0.03	0.97±0.08	3.65±0.30
14.1	...	0.30±0.02	0.72±0.06	2.43±0.21

	Ag	Au	U
3.24	20.9 ±2.2	30.2 ±2.1	34.2 ±2.5
4.09	17.9 ±1.8	27.4 ±1.9	29.5 ±2.1
6.08	12.9 ±1.1	20.6 ±1.4	22.8 ±1.6
10.1	7.35±0.56	12.7 ±0.9	13.6 ±1.0
14.1	4.83±0.42	8.54±0.57	8.96±0.82

Fig. 8 as a function of incident energy. For comparison, data of previous authors including a part of those of Dressel are cited in this figure. The present data, joined smoothly with those of Wright and Trump[2] and of Harder and Ferbert,[18] favor the lower values reported prior to Dressel's.

C. Errors

Possible sources of systematic errors and their values estimated are as follows:

(1) correction factor of Faraday chamber efficiency and the assumption that the multiplication factor f of the ionization chamber was a function of a single variable $\bar{E}$: ±2.9–8.1% error for f, depending on E_0 and Z.

(2) difference of effective solid angle from the calculated one due to possible error in the distance from the target to the collimator, the edge effect of the collimator, and finitenesses of collimator length and area on the target face from which backscattered electrons come out: ±1.8% error for ω;

(3) possible change of secondary-emission coefficient δ during electron bombardment: ±10% error for δ;

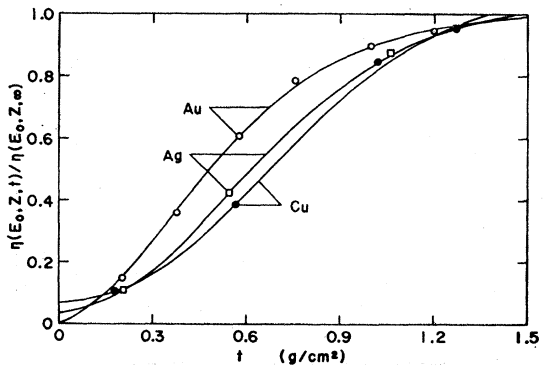

FIG. 7. Dependence of relative backscattering coefficient $\eta(E_0, Z, t)/\eta(E_0, Z, \infty)$ upon thickness t. The incident energy E_0 is 6.08 MeV. The curves represent the least-squares fit of an empirical equation given by Koral and Cohen (Ref. 13, see Sec. IV B1).

(4) unmeasured fraction of background: ±1% error for $I_i(\theta)$ (see Sec. IIF);

(5) secondary emission from the target caused by bremsstrahlung (Sec. IIG), and re-backscattering of electrons from the walls of the scattering chamber to the target: ±0.5% error for I_t;

(6) accuracy of relative indication of the current integrators and the picoammeter: ±1.5% error for $I_i(\theta)/I_t$.

Totals of these errors are listed in Tables I and II for the case of semi-infinite targets. Relative errors in the differential backscattering coefficients for thin targets are about the same as those for the semi-infinite targets of respective atomic numbers at $E_0 = 6.08$ MeV.

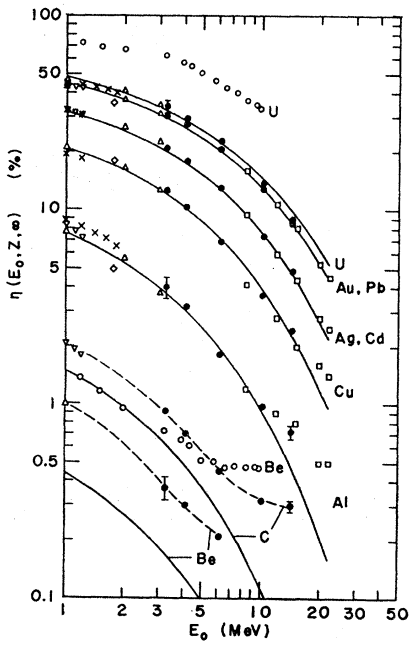

FIG. 8. Dependence of total backscattering coefficient $\eta(E_0, Z, \infty)$ for semi-infinite targets upon incident energy E_0. Possible systematic errors are indicated for representative points of the present data. To avoid confusion, Dressel's results were cited only for Be and U. For other targets also there are similar discrepancy between the data of Dressel and other authors. The solid curves show the relation given by Eq. (12) of Sec. IV B3, and the dashed curves were drawn to connect experimental data for Be and C. ◇ Frank, Ref. 10; △ Wright and Trump, Ref. 2; ▽ Glazunov and Guglya, Ref. 12; □ Harder and Ferbert, Ref. 18; × Cohen and Koral, Ref. 11; ○ Dressel, Ref. 8; ● present data.

IV. DISCUSSION

A. Angular Distribution

1. *Discrepancy in θ_h for $Z \leq 13$*

The values of θ_h for $Z \leq 13$ obtained in the present experiment are generally smaller than those of Dressel, as described in the previous section. In order to estimate the differential backscattering coefficient at 180°, Dressel used a technique of oblique incidence involving

some assumptions. The resulting angular distributions show nonzero gradient at 180° for $Z \leq 13$; this fact suggests that the assumptions used are invalid for these cases and that θ_h shows erroneously large values. Therefore, the invalidity of these assumptions is considered to be the cause of the discrepancy. However, there remains a possibility that the discrepancy can be attributed to a different cause, since values of the backscattering coefficient also show disagreement.

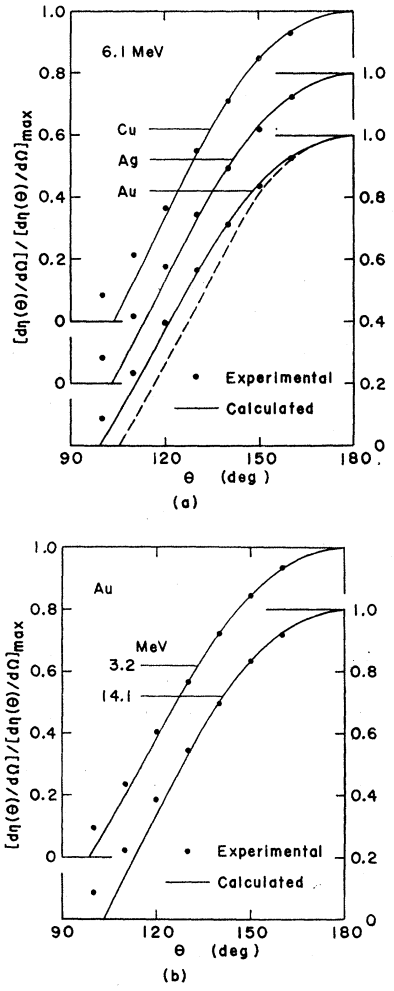

FIG. 9. Experimental and calculated angular distributions of backscattered electrons from semi-infinite targets. The dashed curve in (a) shows the result calculated for Au by using x_0 instead of x_c.

2. *Comparison with a Simple Calculation*

The author has proposed[20] an approach to calculating the angular distribution of backscattered electrons by considering the probability of electrons emerging from effective reflection points (ERP) in the target. Under the simplifying assumption that reflection occurs isotropically at each ERP (diffusion approximation), the angular distribution may be represented approximately by the integral (see Appendix B)

$$d\eta(\theta)/d\Omega = C\int_{x_c/2}^{x_{max}} \exp[-x/\lambda(x,\theta)\cos(\pi-\theta)]dx, \quad (8)$$

where

$$\lambda(x,\theta) = \lambda_0\{1-[1+1/2\cos(\pi-\theta)](x/R)\}, \quad (9)$$

C = a factor independent of θ, x_c = depth of complete diffusion, x_{max} = the smaller of the target thickness and the value of x satisfying $\lambda(x,\theta)=0$, R = practical range of incident electrons, and λ_0 = transport mean free path of incident electrons given by[3]

$$\lambda_0 = \left[2\pi N\int_0^{\pi}\sigma(E_0,Z,\theta)(1-\cos\theta)\sin\theta d\theta\right]^{-1}, \quad (10)$$

where N = the number of scattering atoms per unit volume, and $\sigma(E_0, Z, \theta)$ = scattering cross section for deflection of electrons of kinetic energy E_0 through the angle θ.

In fitting Eq. (8) to the experimental data the value of C is determined so as to normalize the calculated distribution to the experimental one at 180°. Further, x_c is used here as an adjustable parameter, whose value

TABLE III. Values of parameters R, λ_0, and x_c used for the calculation of angular distribution.

Target	E_0 (MeV)	Parameter R (g/cm²)	λ_0 (g/cm²)	x_c (g/cm²)
Cu	6.1	3.0	3.15	1.19
Ag	6.1	2.8	1.84	0.908
Au	3.2	1.5	0.391	0.210
Au	6.1	2.6	1.02	0.528
Au	14.1	4.6	3.53	1.61

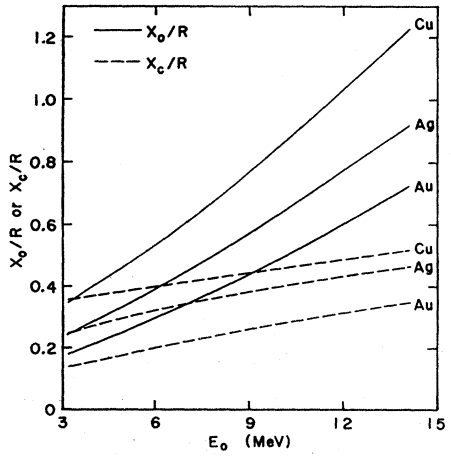

FIG. 10. Dependence of x_c/R and x_0/R upon incident-electron energy E_0.

[20] T. Tabata and S. Okabe, preliminary report to the 20th meeting of the Physical Society of Japan, 1965, p. 156 (unpublished).

TABLE IV. Values of parameters in the empirical relation between backscattering coefficient and target thickness.

	Present data (E_0=6.08 MeV)			Koral and Cohen[a] (E_0=0.6–1.8 MeV)		
Z	α	n	a	α	n	a
26	...	...	...	4.81	2.11	0.015
29	3.1	2.18	0.078	...	...	...
47	3.0	1.92	0.037	6.82	1.92	0.005
79	3.5	1.65	0	8.58	1.65	0

[a] Reference 13.

is determined so that the calculated and experimental values of the ratio $[d\eta(135°)/d\Omega]/[d\eta(180°)/d\Omega]$ for the semi-infinite target may coincide with each other. Examples of angular distributions calculated with this method for semi-infinite targets of $Z\geq 29$ are compared with experimental results in Fig. 9. The values of the parameters used for the calculation are listed in Table III. The values of R were obtained from the works of Hereford and Swann[21] and Noda[22] and those of λ_0, from the approximate expression given by Thümmel.[3] In these examples the agreement of calculated distributions with experimental ones is rather good for $\theta\geq 130°$. It should be noted that the contribution of the electrons incompletely diffused and reflected from the shallow region of the target was neglected in the present calculation on account of the diffusion approximation. This contribution is called here the "sidescattering component" after Seliger[23]; it may be subdivided into single, double, and multiple scattering contributions.[24]

When the above treatment is a good approximation, values of x_c determined to fit Eq. (8) to the experimental data should be consistent with the depth of complete diffusion x_0 expected from the angular distribution of electrons transmitted through a foil (see Appendix C). Though "the depth of complete diffusion" is not a sharply definable quantity, some qualitative conclusions may be drawn from a comparison. In Fig. 10, x_c/R is plotted versus E_0, together with x_0/R. While the two quantities are close to each other near 3 MeV as expected, the difference between them increases with increasing E_0. When x_0 is used instead of x_c in the case of $x_0>x_c$, the angular distribution calculated becomes too narrow, as shown in Fig. 9(a) with a dashed curve. These facts suggest the possibility that x_c as determined was smaller than the proper value at higher energies, thus partially compensating the neglected effect of the sidescattering contribution. An interpretation that this contribution must be taken into account in an improved calculation with increasing weight as E_0 is increased is also possible. This seems to be supported by the fact that the discrepancy between the experimental and calculated results in the region $\theta\leq 120°$ is larger at 14.1 MeV than at 3.2 MeV, as can be seen from Fig. 9(b). Then it is considered that the approximate constancy of angular distribution shapes as a function of energy for $Z\geq 29$ is the result of following compensating tendencies: increase with energy of the relative contribution of the sidescattering component, which broadens the distribution, and narrowing of the distribution of the diffusion component with increasing energy. Calculation with the present approximation cannot be expected to give satisfactory results for the cases of $Z\leq 13$ in the present energy region, because the experimental values of θ_h become appreciably smaller, suggesting the predominance of the former tendency.

Using a modified diffusion theory, Thümmel[24] has recently calculated the contribution of the diffusion component to the total backscattering coefficient, and has found that it is about 50, 70, and 80% for energies 0.1, 0.7, and 4.0 MeV, respectively, in the case of $Z>10$. When this result is combined with the aforementioned consideration, the contribution of diffusion is expected to have a maximum at about a few MeV.

In order to test the present approximation further, it may serve to compare experimental and calculated angular distributions for thin targets. Calculated results for Au at E_0=6.1 MeV are shown in Fig. 3(c), and the calculated value of θ_h for the same case is shown as a function of t in Fig. 4. Quantitatively there is a slight discrepancy between the experimental and calculated results. However, the trend of variation in the experimental data is rather well reproduced with this simple calculation.

From these comparisons it has been found that the calculation based on Eq. (8) can account for some features of the angular distribution. The same approach may possibly give more accurate results for general cases if adequate expressions are derived for the functions $g(x)$ and $h(x, \theta)$ in Eq. (A1) of Appendix B.

B. Total Backscattering Coefficient

1. Dependence on Thickness

Koral and Cohen[13] obtained the following empirical equation for the dependence of relative backscattering coefficient on target thickness:

$$\eta(E_0, Z, t)/\eta(E_0, Z, \infty)=1-\exp[-\alpha(2t/R)^n]+a, \tag{11}$$

where α, n, and a are parameters independent of E_0 in the energy region 0.6–1.8 MeV but dependent on Z. The same equation has been applied to the present data obtained at E_0=6.08 MeV, and the values of the parameters have been determined by using the values of R in Table III. The results are compared in Table IV with those of Koral and Cohen. The constancy of n can be seen to hold up to the present energy; on the

[21] F. L. Hereford and C. P. Swann, Phys. Rev. **78**, 727 (1950).
[22] H. Noda, Nippon Acta Rad. **24**, 387 (1964).
[23] H. H. Seliger, Phys. Rev. **88**, 408 (1952).
[24] H.-W. Thümmel, Z. Physik **198**, 263 (1967).

other hand, the values of α and a show differences between the two results. Curves of Eq. (11) with constants obtained for 6.08 MeV are shown in Fig. 7. The faster rise of these curves for higher-Z targets was explained by Koral and Cohen as due to the higher cross section for Coulomb scattering causing more reversal of direction per penetration of the electrons into the target. For the same reason, the rise of the curve for 0.6–1.8 MeV (when the abscissa is taken as thickness relative to R) is faster than that for 6.08 MeV in the case of the same Z. For example, the thickness of the Au target at which the relative backscattering coefficient becomes $\frac{1}{2}$ is $0.11R$ and $0.19R$ for 0.6–1.8 MeV and 6.08 MeV, respectively, this fact being reflected by the change in the value of the parameter α.

The relative backscattering coefficients measured by Cohen and Koral[11] at the lowest relative thickness ($2t/R \sim 0.04$) level off toward a nonzero intercept for low-Z targets; the same tendency was observed also in the present experiment, as can be seen from Fig. 7. This tendency is considered to be explained by the contribution of energetic secondary electrons. Since the yield of these electrons, most of which have energies in the keV region,[25] is expected to reach a saturated value at a rather small thickness t_s, an extrapolation of relative backscattering coefficient through data for $t > t_s$ may well give a nonzero intercept. Then the parameter a is interpreted as giving approximately the ratio of the number of energetic secondary electrons to the number of backscattered electrons from the semi-infinite target.

2. *Discrepancy in* $\eta(E_0, Z, \infty)$

The total backscattering coefficients $\eta(E_0, Z, \infty)$ for semi-infinite targets obtained in the present experiment favor the lower values reported earlier than Dressel's as described before. The fact that, excepting Dressel's, the results of various workers obtained with different methods come close together may be interpreted as showing the reliability of the lower values. The invalidity for lower-Z targets of the assumptions used by Dressel to estimate the differential backscattering coefficient at 180° may also have caused an error in the total backscattering coefficient. The main cause of the discrepancy, however, should be ascribed to a factor affecting measurements for all the targets. The following points in Dressel's experiment are considered as possible causes:

(1) Efficiency of the beam current monitor. Since Dressel himself reported[26] that the monitor used in his experiment was sensitive to beam conditions such as position and bunch dimensions, the assumption that the efficiency was the same under the conditions for calibration and for the backscattering measurement may have introduced an error.

(2) Solid angle of detection. There is a possibility that some discrepancy existed between the calculated and effective values of solid angle defined by the graphite collimator. The edge effect, increasing the effective solid angle, is expected to be larger for material of lower density.

(3) Effect of stray x rays from the accelerator. These x rays eject secondary electrons from the target, which are indistinguishable from backscattered electrons. A nonanalyzed beam is more likely to give rise to this effect than an analyzed beam.

(4) Effect of target bremsstrahlung on the detector. Though Dressel examined the background without the target and also with it placed at the extreme end of the scattering chamber, there was no consideration of the background due to bremsstrahlung x rays from the target placed at the normal position. In the present experiment the background due to target bremsstrahlung was found to appear in the Faraday chamber as a current of the sense corresponding to a net collection of electrons, and amounted to more than 10% of the signal in the most unfavorable case. This erroneous net collection of electrons is considered to happen when more electrons are emitted by bremsstrahlung from the container walls of the Faraday chamber than from the charge collector. This is the opposite situation to the one considered by Dressel; he discussed only possible charge loss, due to bremsstrahlung, from the collector cups used by previous authors.

The design of the Faraday chamber in the present experiment differed from that of the Faraday cup used by Dressel in the following respects: The charge collector had, not a cup-shaped entrance, but a flat surface, and it was not surrounded by a lead backing. The use of the flat surface necessitated the correction to tht efficiency described in Sec. II E. In determining this correction factor, the lower values of the backscattering coefficient for Al were used. Though the use of Dressel's values increases the result for η(3.24 MeV, 79, ∞), for example, from 30.2 to 31.2%, this value still shows a large discrepancy against his result of η(3.20 MeV, 82, ∞) = 58.9%. The absence of lead backing in the present charge collector cannot be considered to give an important error, since the electron emission due to bremsstrahlung produced in the collector was measured to be less than 0.5% of the collector current. It is to be noted that any of the possible causes (2)–(4), if it had an appreciable effect, would have caused an increase in the measured backscattering coefficients.

3. *Empirical Equation for* $\eta(E_0, Z, \infty)$

Frank[10] predicted that the backscattering coefficient might be a function of a single variable Z/E_0 for $E_0 \gtrsim 1$ MeV. Harder[27] reported that various quantities concerned in the problem of transport of electrons

[25] J. A. Sawyer, J. Appl. Phys. **35**, 1706 (1964).
[26] R. W. Dressel, Nucl. Instr. Methods **24**, 61 (1963).
[27] D. Harder, Biophysik **2**, 381 (1965).

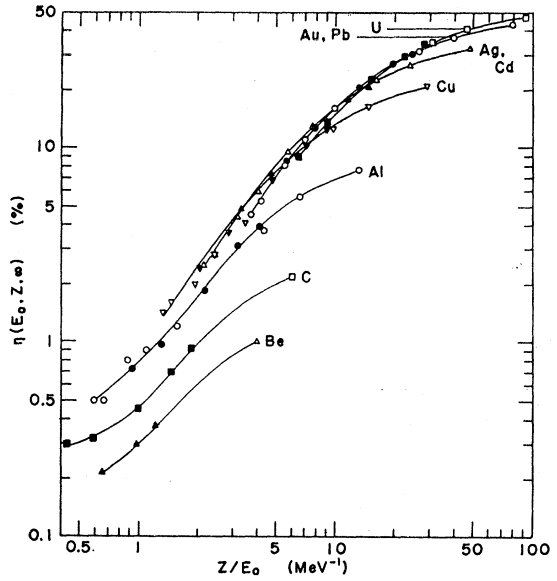

FIG. 11. Plot of total backscattering coefficient $\eta(E_0, Z, \infty)$ for semi-infinite targets as a function of Z/E_0. Open symbols represent the data of Wright and Trump (Ref. 2) and of Harder and Ferbert (Ref. 18), excepting the data for C, which were taken from Glazunov and Guglya (Ref. 12); and solid symbols represent present data. Curves were drawn to get smoothed values.

through bulk matter might approximately be expressed as a function of Z/E_0 for E_0 much higher than the rest energy of the electron. Figure 11 shows the total backscattering coefficient $\eta(E_0, Z, \infty)$ as a function of Z/E_0. There can be seen a tendency for the curves for different Z to approach a single curve as Z/E_0 is decreased. In particular, values for $Z/E_0 \lesssim 10$ MeV^{-1} and $Z \geq 29$ are distributed in a narrow region around the single curve, showing approximate validity of the above predictions in these restricted cases. From an inspection of this plot the following empirical relation can be found:

$$\eta(E_0, Z, \infty) = 1.28 \exp[-11.9Z^{-0.65} \times (1+0.103Z^{0.37}E_0^{0.65})], \quad (12)$$

where E_0 is measured in MeV. This relation is shown in Fig. 8 with solid curves. Its agreement with experimental data for incident energies 1–22 MeV is good except for the cases of $Z \leq 6$ and $Z/E_0 \lesssim 2$ MeV^{-1}. The deviation becomes appreciable only for rather small values of backscattering coefficient ($\lesssim 2\%$), the experimental data lying above the curves of this relation in these cases. This fact suggests the possibility that agreement would be obtained with the same form of equation for more complete regions of Z and E_0 after subtracting the contribution of energetic secondary electrons from the experimental data. It is left as a further problem to find the meaning of the functional form of Eq. (12) and of the values of the constants in it.

V. CONCLUSION

The differential and the total backscattering coefficients of electrons were obtained for semi-infinite targets of atomic numbers 4–92 in the incident energy range 3.24–14.1 MeV, and similar data were obtained for Cu, Ag, and Au targets of various thicknesses at the energy of 6.08 MeV. The broadening of the angular distribution for $Z \leq 13$ with increasing energy in the present region is considered to indicate the increasing relative contribution of sidescattered electrons compared with back-diffused electrons. Though the angular distribution shapes for $Z \geq 29$ remain almost constant with varying energy, a comparison with the simple calculation has suggested that the relative contribution of the sidescattering process increases with increasing energy also for these atomic numbers. The nonzero intercept obtained upon extrapolation of the relative backscattering coefficient to zero thickness for lower-Z targets was interpreted as caused by the contribution of energetic secondary electrons. The values of the total backscattering coefficient observed favor the lower values reported before Dressel's. The approach proposed for the calculation of angular distribution and the empirical equation found for $\eta(E_0, Z, \infty)$ may be of use for further investigations of the backscattering in the MeV region.

ACKNOWLEDGMENTS

The author would like to express his appreciation to President K. Kimura and Dr. T. Azuma for their advice and encouragement throughout the course of this research. He would also like to thank Dr. S. Okabe for his stimulating discussions and suggestions on the various aspects of the work, and R. Ito for his assistance in performing the experiment. Thanks are due to Dr. D. Harder for his kind communications. Finally the author wishes to thank K. Tsumori and other members of the linear accelerator group of this laboratory for their valuable help in the operation of the machine.

APPENDIX A

Wright and Trump[2] have reported the average energy $\bar{E}(E_0, Z)$ per electron backscattered into the backward hemisphere for Al, Cu, and Pb targets in the energy range of incident electrons 1–3 MeV. The present author and his co-workers[28] have performed a measurement of the average energy per electron backscattered in the direction of 160° for a Au target in the energy range 3.2–14 MeV. Both results show that the ratio of average energy to incident energy decreases with increasing incident energy in these regions almost linearly in a plot with logarithmic scales. On the basis of this fact, the values of $\bar{E}(E_0, Z)$ in the case of the present incident energies were obtained for Al, Cu, and Pb

[28] T. Tabata, S. Okabe, and R. Ito (unpublished).

through a linear extrapolation in this plot of the result of Wright and Trump; values for other targets were determined through an interpolation or extrapolation in atomic number. The values used varied from 1.2 MeV for $E_0=3.2$ MeV and $Z=4$ to 6.1 MeV for $E_0=14$ MeV and $Z=92$.

APPENDIX B

In this Appendix, considerations underlying Eqs. (8) and (9) of Sec. IV A2 are described.

Let us consider a uniform flux of monoenergetic electrons normally incident on the plane surface of the solid target. An effective reflection point (ERP) can be defined for each of the backscattered electrons escaping from this surface. When iterated returns are made by the electron, the average depth of points where reflection toward the back has taken place can be regarded as the depth of the ERP. The probability that the electron returning in the direction θ from the ERP at the depth x will emerge from the surface is considered to be given by $\exp[-x/\lambda(x,\ \theta)\ \cos(\pi-\theta)]$, where $\lambda(x, \theta)$ is the effective transport mean free path of the electron during the backward travel. The statistical behavior of electrons in the target causes a distribution $g(x)$ of ERP along the depth, and the ERP at each depth reflects electrons with an angular distribution $h(x, \theta)$. Therefore, the number of electrons, per incident electron, outgoing from the surface into the solid angle $d\Omega$ at θ is given by

$$d\eta(\theta)=C\int_0^{x_{\max}} g(x)h(x,\theta)\ \exp[-x/\lambda(x,\theta)\times\cos(\pi-\theta)]dxd\Omega, \quad \text{(B1)}$$

where C is a factor independent of θ.

In evaluating this integral, some approximate expressions are required for the functions $g(x)$, $h(x, \theta)$, and $\lambda(x, \theta)$. The most simple approximation is to regard all these functions as constants. Letting $x_{\max}$ go to infinity in this approximation, we get

$$d\eta(\theta)\propto\cos(\pi-\theta)d\Omega, \quad \text{(B2)}$$

which is frequently mentioned as the distribution of diffusing electrons emerging from the plane surface. In order to improve the approximation it is necessary to find more suitable forms for these functions.

Some successes of diffusion theory suggest that electrons can be considered to reach a state of complete diffusion at some depth x_c. In this state electrons almost entirely lose their initial direction of motion. Then $h(x, \theta)$ becomes a constant for $x\geq x_c$. If we assume that the main contribution of backscattered electrons is composed of those electrons reflected after reaching the state of complete diffusion, $g(x)$ is expected to be a function that increases from zero at $x=0$ to a maximum somewhere in the region $x\gtrsim x_c$, and decreases to zero at the maximum range of incident electrons. For simplicity it may be approximated by

$$\begin{aligned} g(x)&=0, \quad x<x_c/2 \\ &=1, \quad x_c/2\leq x\leq x_{\max}. \end{aligned} \quad \text{(B3)}$$

Moreover, the diffusion approximation permits us to regard $h(x, \theta)$ as a constant over the whole depth. Then Eq. (B1) takes the form given by Eq. (8). In Eq. (9) a simple linear decrease of mean free path with increasing traversed depth is assumed, and the value at the midpoint of the return path is employed for $\lambda(x, \theta)$.

APPENDIX C

Bethe *et al.*[29] defined the depth of complete diffusion as the depth at which the average cosine of the angle between the actual direction of motion and the direction of the primary beam becomes $1/e$. For the purpose of simple evaluation, a semiempirical estimation of the diffusion depth is made here.

Let us consider the angular distribution of electrons transmitted through a foil. According to Hanson *et al.*,[30] the half-width of this angular distribution, defined as the angle θ_w at which the distribution function has fallen to $\frac{1}{2}$ of its maximum, is given by the following equation:

$$\theta_w=0.833\theta_1(B-1.2)^{1/2}, \quad \text{(C1)}$$

where

$$\theta_1=(22.9\ \text{MeV}/pv)[Z(Z+1)x/A\ (\text{g/cm}^2)]^{1/2}. \quad \text{(C2)}$$

Values of B are tabulated by Molière[31]; p and v are the momentum and the velocity, respectively, of electrons, x is the thickness of the foil, and A is the atomic weight of the foil material. Frank[10] found experimentally that for the incident electrons of 1.75-MeV energy, θ_w no longer varies much with x for $x\gtrsim x_0$, where x_0 is the thickness giving $\theta_w=45°$ in Eq. (A4). The present author and his co-workers[32] have found the same fact for energies up to 14 MeV. Therefore, x_0 can be considered to give an estimate of the depth of complete diffusion.

[29] H. A. Bethe, M. E. Rose, and L. P. Smith, Proc. Am. Phil. Soc. **78**, 573 (1938).
[30] A. O. Hanson, L. H. Lanzl, E. M. Lyman, and M. B. Scott, Phys. Rev. **84**, 634 (1951).
[31] G. Molière, Z. Naturforsch. **3a**, 78 (1948).
[32] T. Tabata, S. Okabe, and R. Ito (unpublished).